Journal Pre-proof

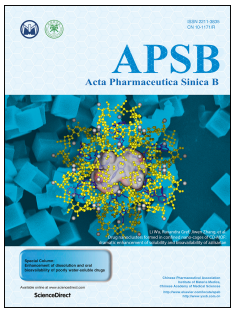

mRNA display-enabled discovery of proximity-triggered covalent peptide–drug conjugates

Ruixuan Wang, Siqi Ran, Jiabei Guo, Da Hu, Xiang Feng, Jixia zhou, Zhanzhi Zhang, Futian Liang, Jiamin Shang, Lingxin Bu, Kaiyi Wang, Junyi Mao, Huixin Luo, Rui Wang

PII: S2211-3835(25)00507-6

DOI: https://doi.org/10.1016/j.apsb.2025.07.029

Reference: APSB 2474

To appear in: *Acta Pharmaceutica Sinica B*

Received Date: 27 June 2025

Revised Date: 13 July 2025

Accepted Date: 14 July 2025

Please cite this article as: Wang R, Ran S, Guo J, Hu D, Feng X, zhou J, Zhang Z, Liang F, Shang J, Bu L, Wang K, Mao J, Luo H, Wang R, mRNA display-enabled discovery of proximity-triggered covalent peptide–drug conjugates, *Acta Pharmaceutica Sinica B*, https://doi.org/10.1016/j.apsb.2025.07.029.

Short communication

mRNA display-enabled discovery of proximity-triggered covalent peptide–drug conjugates

Ruixuan Wang[a,†], Siqi Ran[a,†], Jiabei Guo[a,†], Da Hu[a,†], Xiang Feng[a], Jixia zhou[a], Zhanzhi Zhang[a], Futian Liang[a], Jiamin Shang[a], Lingxin Bu[a], Kaiyi Wang[a], Junyi Mao[a], Huixin Luo[a,*], Rui Wang[a,b,*]

[a]*State Key Laboratory of Bioactive Substance and Function of Natural Medicines, Institute of Materia Medica, Chinese Academy of Medical Sciences and Peking Union Medical College, Beijing 100050, China*

[b]*Key Laboratory of Preclinical Study for New Drugs of Gansu Province, School of Basic Medical Sciences and Research Unit of Peptide Science, Chinese Academy of Medical Sciences, Lanzhou University, Lanzhou 730000, China*

Received 27 June 2025; received in revised form 13 July 2025; accepted 14 July 2025

[*]Corresponding authors.

E-mail addresses: luohuixin@imm.ac.cn (Huixin Luo), wangrui@lzu.edu.cn (Rui Wang).

[†]These authors made equal contributions to this work.

Running title: mRNA display discovery of covalent PDCs

Graphical abstract

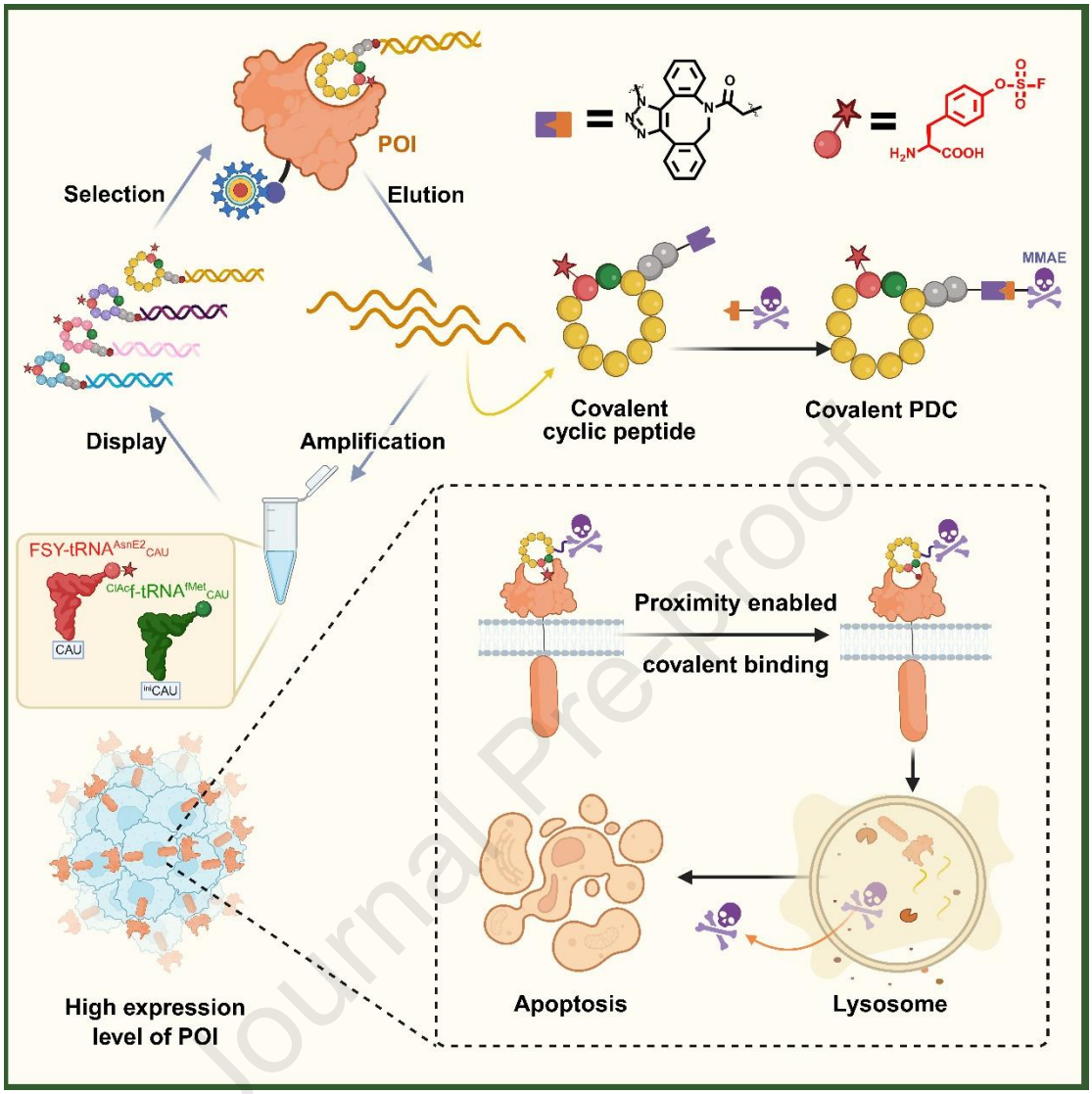

This study presents an mRNA display platform that combines covalent warhead encoding with macrocycle libraries and screens covalent cyclic peptides aimed at Nectin-4. Using these peptides, the authors produced covalent PDCs that demonstrated significant cytotoxicity against MDA-MB-468 cells.

Short communication

mRNA display-enabled discovery of proximity-triggered covalent peptide–drug conjugates

Ruixuan Wang[a,†], Siqi Ran[a,†], Jiabei Guo[a,†], Da Hu[a,†], Xiang Feng[a], Jixia zhou[a], Zhanzhi Zhang[a], Futian Liang[a], Jiamin Shang[a], Lingxin Bu[a], Kaiyi Wang[a], Junyi Mao[a], Huixin Luo[a,*], Rui Wang[a,b,*]

[a]*State Key Laboratory of Bioactive Substance and Function of Natural Medicines, Institute of Materia Medica, Chinese Academy of Medical Sciences and Peking Union Medical College, Beijing 100050, China*

[b]*Key Laboratory of Preclinical Study for New Drugs of Gansu Province, School of Basic Medical Sciences and Research Unit of Peptide Science, Chinese Academy of Medical Sciences, Lanzhou University, Lanzhou 730000, China*

Received 27 June 2025; received in revised form 13 July 2025; accepted 14 July 2025

[*]Corresponding authors.

E-mail addresses: luohuixin@imm.ac.cn (Huixin Luo), wangrui@lzu.edu.cn (Rui Wang).

[†]These authors made equal contributions to this work.

Running title: mRNA display discovery of covalent PDCs

Abstract Peptide–drug conjugates (PDCs) have emerged as a promising modality in precision oncology, enabling targeted delivery of cytotoxic payloads while minimizing off-target toxicity. The integration of covalent warheads, such as those based on sulfur(VI) fluoride exchange (SuFEx) chemistry, enhances drug–target residence time and tumor accumulation. However, existing screening methods for covalent peptide (CP) libraries require post-translational warhead conjugation, limiting throughput. Here, we present an integrated mRNA display platform that incorporates covalent warheads during ribosomal synthesis, enabling efficient screening of ultra-diverse covalent macrocyclic peptide libraries (>10^{13} variants). This approach, using site-specific incorporation of *N*-chloroacetyl-D-phenylalanine and fluorosulfate-L-tyrosine,

accelerated the discovery of irreversibly binding (K_i = 3.58 μmol/L) Nectin-4-targeting peptide CP-N1-N_3 *via* proximity-triggered SuFEx. The peptide was further conjugated to cytotoxic payloads, yielding the covalent PDC CP-N1-MMAE with potent cytotoxicity (IC_{50} ≈ 43 nmol/L) against MDA-MB-468 cells. This platform establishes a new paradigm for precision covalent drug discovery.

KEY WORDS Covalent peptide; Macrocyclic peptide; mRNA display; Flexizyme; Nectin-4; Sulfur(VI) fluoride exchange; Fluorosulfate-L-tyrosine; Peptide–drug conjugate

1. Introduction

Peptide–drug conjugates (PDCs) have emerged as a promising approach in precision oncology, facilitating specific delivery of cytotoxic agents while reducing off-target damage[1]. The development of novel peptide ligands with high affinity, selectivity, and enhanced pharmacokinetics has been the primary focus of research to enhance efficacy[2]. The addition of covalent warheads into PDCs enables the creation of irreversible drug–target complexes, hence extending the target's residence duration and improving tumor-specific accumulation *via* receptor-mediated endocytosis[3]. The latest developments in sulfur(VI) fluoride exchange (SuFEx) chemistry offer distinct benefits for warhead design: its sulfonyl fluorine group remains inert in physiological conditions and activates covalent binding only upon proximity to specific nucleophilic residues of the target, achieving an optimal equilibrium between stability and bioorthogonality[4-6]. Despite the advancements in structure-based drug design that have enabled the application of sulfonyl fluoride therapeutic agents across several modalities (small molecules, biologics, and nucleic acids)[7-11], a universal methodology is still required to directly screen extensive ligand libraries for their ability to establish covalent and selective protein-ligand interactions.

Recent studies have sought to utilize peptide libraries containing covalent warheads for direct screening[12-14]. Nevertheless, these strategies typically depend on the warhead conjugation process following phage display, which considerably raises

screening complexity and restricts throughput. Conversely, mRNA display technology has shown its special significance in using cell-free translation systems to build a hyperdiverse peptide library (>10^{13} variants) and engineering a flexible enzyme (flexizyme) that incorporates covalent warheads during translation[15-17]. Various unnatural amino acids with covalent warheads are introduced into the peptide-mRNA/cDNA complex, for example dehydroalanine and *p*-benzoyl-L-phenylalanine. The *in situ* integration strategy eliminates the necessity for further chemical modifications and establishes an innovative platform for the efficient discovery of highly selective covalent PDCs.

This report presents the development of an mRNA display platform that combines a covalent warhead encoding strategy with diverse macrocycle libraries, facilitating the identification of optimal irreversible binders for target proteins (Fig. 1). The libraries were constructed by incorporating *N*-chloroacetyl-D-phenylalanine (^{ClAc}f) at the initiator and fluorosulfate-L-tyrosine (FSY) during the process of translation elongation. We conducted a proof-of-concept demonstration by screening covalent macrocyclic peptides that target Nectin-4, confirming their specific and efficient covalent interaction with cells exhibiting high Nectin-4 expression. The best candidate peptide CP-N1-N_3 demonstrated a great binding affinity (K_i = 3.58 μmol/L) and facilitated irreversible covalent conjugation to Nectin-4 through SuFEx click reaction on the cell surface. Based on these findings, we designed and synthesized peptide–drug conjugate (PDC)—CP-N1-MMAE, using copper-free strain promoted azide-alkyne cycloaddition (SPAAC) chemistry. This covalent PDC exhibited strong covalent binding to MDA-MB-468 cells and displayed significant cytotoxicity (IC_{50} ≈ 43 nmol/L), effectively inducing cancer cell death. The findings underscore the therapeutic promise of covalent PDC as advanced Nectin-4-targeted anticancer agents, demonstrating improved target specificity and efficacy. The integrated screening platform presented here provides an effective strategy for identifying covalent macrocyclic peptide drugs targeting various therapeutic areas, thereby establishing a model for precision covalent drug development.

2. Results and discussion

2.1. Design and selection of covalent mRNA display library to Nectin-4

To establish a universal methodology for covalent peptide (CP) screening, we integrated the sulfonyl fluorine warhead into the mRNA display strategy (Fig. 1). This warhead serves as an optimal reactive electrophile for chemical modification due to its ability to target multiple nucleophilic residues—notably tyrosine (Tyr), histidine (His), and lysine (Lys)—*via* SuFEx click chemistry[18]. FSY, a side chain-modified tyrosine analogue extensively utilized in covalent protein engineering through genetic codon expansion (GCE) in *Escherichia coli* and mammalian cells[18-20], promised to serve as a covalent building block for incorporating the fluorosulfate group into ribosomally synthesized peptides. We designed and synthesized fluorosulfate-L-tyrosine cyanomethyl ester (FSY-CME) as a substrate for the flexible *in vitro* translation (FIT) system[17] (Fig. 2A and B). This compound can be enzymatically charged onto the optimized unnatural $tRNA^{AsnE2}_{CAU}$ by flexizyme eFx, forming unnatural aminoacyl-tRNA FSY-$tRNA^{AsnE2}_{CAU}$ (Fig. 2A). Concurrently, we designed another FIT substrate, *N*-chloroacetyl-D-phenylalanine cyanomethyl ester (^{ClAc}f-CME), for aminoacylation to $tRNA^{fMet}_{CAU}$ which only recognized the initial AUG codon (Fig. 2B). Incorporation of *N*-chloroacetyl-D-phenylalanine (^{ClAc}f) at the first position by adding ^{ClAc}f-$tRNA^{fMet}_{CAU}$ enables reaction with a designed downstream cysteine residue to form a thioester bond for peptide cyclization (Fig. 2A). Microhelix RNA assays confirmed aminoacylation efficiencies of approximately 80% and 40% for ^{ClAc}f and FSY, respectively (Fig. 2C). To validate site-specific incorporation during in *vitro* translation, we designed a model mRNA template encoding a hemagglutinin (HA) tag flanked by two direct upstream AUG codons for unnatural amino acid (UAA) insertion. Mass spectrometric analysis confirmed successful FSY incorporation into the target peptides. (Supporting Information Fig. S1A). Using this construct, we adapted an mRNA display-based protocol to enrich full-length products, followed by quantitative polymerase chain reaction (qPCR) detection. This approach revealed a translational efficiency of ~80% for FSY, comparable to that of methionine under identical conditions (Fig. S1B and S1C).

We next engineered high-diversity libraries compatible with mRNA display for *de novo* biopanning of covalent peptide binders. These libraries comprised 8–12 amino acid variable regions encoded by degenerate NNK codons, with the reactive FSY warhead strategically incorporated at random positions through NNK-randomized AUG codons. Additionally, ^{ClAc}f-tRNA$^{fMet}_{CAU}$ was added into ribosomally peptide synthesis system for library cyclization by reaction with downstream designed cysteine residue (Fig. 1). Subsequently, our biopanning workflow leveraged covalent macrocyclic peptide libraries through four optimized steps: (i) *in vitro* translation and ^{ClAc}f-mediated cyclization, (ii) target crosslinking with biotinylated protein and streptavidin capture, (iii) stringent washing (5 mol/L guanidine hydrochloride) to eliminate non-crosslinked species, and (iv) next-generation sequencing (NGS) analysis for enriched binder identification (Fig. 1).

After establishing a method for discovering novel covalent binders, we applied this approach to screen the extracellular domain (ECD) of Nectin-4—a protein overexpressed in multiple cancers, including breast, lung and ovarian malignancies[21]. After six selection rounds, qPCR quantification revealed a significant increase in library enrichment, demonstrating the efficacy of iterative selection (Supporting Information Fig. S2). NGS analysis of the final enriched libraries identified candidate covalent peptide sequences. Among the top 100 peptides ranked by NGS frequency, 62 contained FSY incorporation sites, with 4 peptides incorporating two FSY residues. The highest-ranked candidates dominated the NGS results (>80%) and exhibited significant sequence homology. These peptides consistently incorporated FSY at the second amino acid position and shared the conserved sequence motif “fXNAFPVRxLxxWC” (“f” = D-Phe, “X” = FSY and “x” = variable residues) (Fig. 2D), demonstrating the efficacy of our high-throughput method for identifying covalent macrocyclic peptide binders targeting Nectin-4.

In parallel, we screened for non-covalent Nectin-4 binders using the random non-standard peptides integrated discovery (RaPID) strategy. This involved omitting FSY-tRNA$^{AsnE2}_{CAU}$ during translation and employing milder wash conditions post-affinity

selection (Supporting Information Fig. S3A). Comparatively, DNA recovery also increased significantly after six selection rounds (Fig. S3B). NGS identified potential non-covalent candidates for validation. Top-ranking peptides exhibited partial sequence similarity with covalent candidates, particularly peptide NP-N7, which featured conserved basic residues (Fig. S3C). We synthesized the top 7 candidates and evaluated their binding affinity for Nectin-4 by surface plasmon resonance (SPR). NP-N7 exhibited the strongest binding (K_D = 0.362 μmol/L) (Supporting Information Fig. S4).

After high-throughput screening, we focused on developing a mild and efficient method for orthogonal introduction of sulfonyl fluoride groups to specific tyrosine residues on solid-phase peptide synthesis (SPPS) resins, enabling the synthesis of macrocyclic peptides for downstream functional characterization and therapeutic development (Fig. 2E). Previous work has reported strategies employing orthogonal protecting groups on tyrosine side chains using *o*-nitrobenzyl, allyl, and *tert*-butyldimethylsilane (TBS)[22], as well as sulfonyl fluoride modification and subsequent sulfonic acid derivatization[23]. Motivated by these results, we designed an orthogonal tyrosine-protecting group strategy that facilitated chemoselective modification under mild conditions. Specifically, we prepared resin-bound peptides containing TBDPS (*t*-butyldiphenylsilyl)-protected tyrosine residues *via* Fmoc SPPS. The silyl protecting group was removed under mild conditions using a KF aqueous solution/DMF mixture, followed by introduction of sulfonyl fluoride group at the side chain of specific tyrosine site *via* a *N*-[4-[bis(fluorosulfonyl)amino]phenyl]acetamide (AISF)[24]/ 2,3,4,6,7,8,9,10-octahydropyrimido[1,2-*a*]azepine (DBU) system. The linear peptide was cleaved from the resin with trifluoroacetic acid (TFA), and subsequently cyclized under dilute conditions, yielding head-to-tail macrocyclic peptides (Fig. 2E). We investigated the rationale for selecting TBDPS group as the tyrosine side-chain protecting group (Supporting Information Fig. S5) and optimized the reaction conditions for sulfonyl fluoride installation in small-molecule models (Supporting Information Table S1).

Based on our established routine of peptide modification, we synthesized the top seven candidate peptides with FSY incorporation (Fig. 2D and E). For the continuous

functional modification and extensive applications, we modified their *C*-termini with both polyethylene glycol (PEG) and L-azidonorleucine (K1) (Fig. 2F). The modified azide group served as a versatile handle for subsequent bioconjugation *via* strain-promoted azide-alkyne cycloaddition (SPAAC) click chemistry, facilitating linkage to diverse molecules such as fluorescent dyes or cytotoxic agents. SPR analysis further characterized binding, identifying CP-N1-N_3 (K_D = 2.82 μmol/L) and CP-N9-N_3 (K_D = 6.40 μmol/L) as the tightest binders among the candidates (Supporting Information Fig. S6). Meanwhile, in the single-cycle kinetics experiments with longer binding time (800 s), the binding curves did not return to baseline after washing steps (200 s), which demonstrated the irreversible binding of covalent peptides (Fig. 2G). Fitting by a two-state reaction model, we obtained more accurate values of dissociation constants (CP-N1-N_3: K_i = 3.58 μmol/L; CP-N9-N_3: K_i = 4.94 μmol/L). It also proved that our covalent peptide screening technique provided an effective routine for covalent binder identification.

2.2. Verification of the covalent binding of macrocyclic peptides to Nectin-4

Following screening and synthesis, we sought to experimentally validate the covalent interactions between selected peptides and the target protein. Upon peptide-mediated target engagement, the sulfonyl fluoride warhead reacts *via* SuFEx click chemistry with proximal nucleophilic residues (Tyr, His, Lys), enabling covalent bond formation[18] (Fig. 3A). This proximity-driven ligation mechanism significantly reduces the off-target interactions while ensuring high binding specificity. The sulfur(VI)-fluoride bonds exhibit exceptional stability against biological degradation pathways[18], enabling irreversible target engagement with potential applications in covalent drug discovery[25,26].

Pervious SRP results could validate that covalent crosslinking between Nectin-4 and covalent peptide candidates (Fig. 2G). To confirm the covalent crosslinking effects, we incubated top seven CP candidates (10 μmol/L) with purified Nectin-4 ECD (1 μmol/L). Resulting protein-peptide conjugates were then labeled with

dibenzocyclooctyne-Cy3 (DBCO-Cy3) *via* SPAAC for fluorescent quantification. In-gel fluorescence analysis revealed successful covalent conjugation for six candidates (CP-N1-N_3 to CP-N9-N_3, excluding CP-N8-N_3), with CP-N1-N_3, CP-N4-N_3 and CP-N9-N_3 demonstrating particularly robust labeling efficiency (Fig. 3B). Competition experiments with 5 μmol/L BSA (bovine serum albumin) (5× molar excess over Nectin-4 ECD) showed negligible off-target labeling (<5% signal intensity *vs.* Nectin-4), confirming exceptional target specificity of our covalent peptides (Supporting Information Fig. S7A). We also tested the crosslinking with other members in Nectin family, Nectin-1, 2 and 3, which performed much lower level (about 6 times) of binding of covalent peptides rather than Nectin-4 (Fig. S7B), confirming the high specificity. Beyond labeling efficiency and target specificity, CP-N1-N_3 and CP-N9-N_3 exhibited the most favorable binding kinetics in SPR analysis, with equilibrium dissociation constants (K_i) of 3.58 and 4.94 μmol/L respectively, prompting their selection as lead candidates (Fig. 2G). These peptides share high sequence similarity, differing only at position 12 (lysine in CP-N1-N_3, arginine in CP-N9-N_3). Dose-response profiling (0.8-50 μmol/L) established concentration-dependent Nectin-4 engagement for both leads, with near-identical potency (CP-N1-N_3 EC_{50} = 36 ± 8 μmol/L; CP-N9-N_3 EC_{50} = 33 ± 8 μmol/L) (Fig. 3C and Fig. S7C). Kinetic dissection revealed rapid target engagement, achieving half-maximal labeling within 86 ± 23 min (CP-N1-N_3) and 108 ± 27 min (CP-N9-N_3) (Fig. 3C and Fig. S7C). These results demonstrate that our screening platform successfully identifies the covalent peptides capable of irreversible Nectin-4 engagement *in vitro*, with CP-N1-N_3 and CP-N9-N_3 emerging as optimal candidates due to their combined attributes of exceptional binding kinetics and absolute target specificity.

As a therapeutic target protein, Nectin-4 was overexpressed in various types of cancers[27]. Given Nectin-4's clinical significance in breast and bladder cancer[28], we employed matched breast cancer lines (MDA-MB-468, high expressor; MCF-7, low expressor) to establish target-specific covalent labeling (Supporting Information Fig. S8A). We then synthesized fluorescent probes by conjugating DBCO-Cy3 to the C-

terminal azide of CP-N1-N_3 and CP-N9-N_3 *via* SPAAC click reaction for cell incubation. At 10 μmol/L concentration, both CP-N1-Cy3 and CP-N9-Cy3 exhibited specific subcellular localization patterns co-localizing with Nectin-4, suggesting enhanced target engagement efficiency (Fig. 3D). Consistent with Nectin-4-dependent binding, both peptides exhibited minimal background labeling in MCF-7 cells (Nectin-4 low), with fluorescence intensity reduced by >95% compared to MDA-MB-468 cells (Nectin-4 high), confirming target-specific covalent engagement (Fig. S8B). For comparison, we similarly labeled the high-affinity non-covalent binder NP-N7 (K_D = 0.362 μmol/L) identified *via* RaPID screening. Despite its 10-fold higher affinity than CP-N1/CP-N9, NP-N7-Cy3 exhibited significantly weaker cellular labeling than the covalent probes (Fig. S8B and S8C). This disparity suggested the covalent warhead enhanced target engagement efficiency. To confirm covalent cell-surface attachment, we treated MDA-MB-468 cells with Cy3-labeled peptides followed by stringent washing to disrupt non-covalent interactions. Fluorescence imaging revealed retained binding for CP-N1 and CP-N9 under denaturing conditions, while the NP-N7 signal was completely abolished, demonstrating the covalent stabilization conferred by the FSY warhead (Fig. 3E).

Collectively, we confirm that our screened covalent macrocyclic peptides can conjugate irreversibly with Nectin-4 on the surface of MDA-MB-468 cells, which lays the foundation for us to construct covalent PDCs.

2.3. Evaluation and mechanistic analysis of tumor apoptosis induced by covalent PDCs

Covalent peptides represent a transformative platform for next-generation PDCs[29,30]. We proposed that covalent PDCs achieved target cell killing through a four-step mechanism (Fig. 4A): (i) The peptide ligand selectively identified and irreversibly cross-linked with the target receptor where a reactive warhead forms a covalent bond with specific receptor residues. (ii) Ligand–receptor complexes activated cellular endocytic signaling, resulting in endosome formation. (iii) Endocytic vesicles underwent directed fusion with lysosomes, wherein the linker is hydrolyzed under

enzymatic conditions, culminating in controlled liberation of the therapeutic payload. (iv) The released active drug reached intracellular targets to induce apoptosis[31]. Through covalent modification of macrocyclic peptides, covalent PDCs irreversibly bind to targets, significantly extending target residence time. This combination of efficient internalization and resistance to lysosomal degradation substantially increase intracellular drug concentrations within target cells[32].

As the prerequisite of PDC induced target cell killing, we should validate the internalization of our covalent PDCs. We employed Cy3-conjugated covalent peptides as structurally identical substitutes for the targeting binders. By treatment with a Cy3-conjugated covalent peptides concentration gradient (CP-N1-Cy3 or CP-N9-Cy3, 0.1 to 10 μmol/L), the increasing Cy3 signals demonstrated successful, dose-dependent binding and continuous internalization of MDA-MB-468 cells (Supporting Information Fig. S9A and S9B). Fluorescence imaging revealed marked co-localization of internalized Cy3 signals with lysosomes, confirming that CP-N1-Cy3 or CP-N9-Cy3 entered cells *via* endocytosis (Fig. S9B). We also evaluated the non-covalent peptide NP-N7-Cy3, which exhibited lower endocytosis efficiency (Fig. S9A and S9B). These results prove that the peptide-dye conjugates enter cell by endocytosis, and it provides a mechanistic basis for selective release of our covalent PDCs.

Based on the confirmation of the cell endocytosis, we designed covalent PDCs *via* SPAAC click chemistry. Azide-functionalized CPs were conjugated to DBCO-Val-Cit-PAB-MMAE (monomethyl auristatin E)—a potent tubulin polymerization inhibitor widely used in antibody-drug conjugate (ADC)/PDC payload design, to generate our covalent PDCs, named CP-N1-MMAE and CP-N9-MMAE (Fig. 4A). After cellular internalization, the protease cathepsin B (CTSB) selectively cleaved the Val-Cit-PAB linker within lysosomes, releasing free MMAE molecules into the cytosol to induce apoptosis through microtubule disruption (Fig. 4A).

We subsequently synthesized and purified covalent PDCs, CP-N1-MMAE and CP-N9-MMAE, *via* SPAAC click reaction. We test the stability of covalent PDCs in mouse serum, which CP-N1-MMAE ($t_{1/2}$ = 4.41 h) performed much better than CP-N9-

MMAE ($t_{1/2}$ = 1.19 h) (Supporting Information Fig. S10). To assess cytotoxic potency, we measured cell viability across concentrations (10 nmol/L to 10 μmol/L) in MDA-MB-468 cells. Both conjugates induced a pronounced, concentration-dependent reduction in survival rates, with IC_{50} values of 43.45 ± 4.00 nmol/L (CP-N1-MMAE) and 43.37 ± 4.53 nmol/L (CP-N9-MMAE) (Fig. 4B and Supporting Information Fig. S11A). These low IC_{50} values indicated robust cytotoxicity against Nectin-4-expressing cells. For comparison, the non-covalent PDC NP-N7-MMAE exhibited higher cytotoxic potency (IC_{50} = 8.37 ± 1.32 nmol/L), yet failed to reduce viability below 40% even at high concentrations (Fig. S11B). Under identical conditions, covalent PDCs achieved approximately 80% cell killing. The lower area under the dose-response curve (AUC) (173.3 for CP-N1-MMAE, 215.2 for CP-N9-MMAE and 433.7 for NP-N7-MMAE) of CP-N1-MMAE indicated stronger target cell killing effect (Fig. 4B and Fig. S11). These findings demonstrate the potential of covalent PDCs for efficient target cell killing and highlighted how covalent binding enhanced drug efficacy, especially CP-N1-MMAE.

As a widely used cytotoxic payload in PDCs, MMAE disrupts tubulin assembly and impedes cell cycle progression. To elucidate the cytotoxic mechanisms of our PDCs, MDA-MB-468 cells were treated for 24 h with escalating concentrations (from 0 to 10 μmol/L) of CP-N1-MMAE, CP-N9-MMAE, and NP-N7-MMAE for 24 h. Immunofluorescent imaging revealed a progressive, concentration-dependent reduction in tubulin signal, confirming cell killing *via* tubulin–disruption pathways (Fig. 4C and Supporting Information Fig. S12). We further evaluated apoptosis induction by covalent PDC treatment. Annexin V/PI staining analyzed by flow cytometry showed that 1 μmol/L of both two covalent PDCs led to a marked elevation in the percentage of apoptotic cells (approximately 60%) (Fig. 4D and E and Supporting Information Fig. S13A–S13D), comprising in ~50% early-stage and ~10% late-stage apoptosis (Fig. S13C and S13D). This ratio increased significantly with higher concentrations. Compared to covalent PDCs, NP-N7-MMAE exhibited comparative lower potency and efficacy in inducing apoptosis (Fig. S13B–S13D). Within apoptotic cells triggered by

CP-N1-MMAE, cleavage products of key apoptotic markers caspase-3 and poly ADP-ribose polymerase (PARP) increased to 5- and 1.5-fold, respectively, relative to untreated controls (Fig. 4F). All three PDCs produced similar dose-dependent elevations in these markers, with statistically significant enhancements observed across concentrations (Fig. 4F and Supporting Information Fig. S14). These findings collectively indicate that covalent PDCs eliminate target cells through the tubulin assembly disruption and apoptosis induction.

2.4. Discussion

Covalent drugs, which lock onto targets through permanent covalent tethering, have garnered significant attention in drug development[25]. Compared to established covalent small molecules and protein drugs, covalent peptides offer distinct physicochemical properties and lower production costs, positioning them as a prominent focus in pharmaceutical research. The sulfonyl fluoride warhead employed here undergoes SuFEx click chemistry to covalently engage diverse natural amino acids—including Tyr, His, and Lys—with broad applicability[18]. This proximity-driven reaction operates without exogenous activation, enhancing its drug development potential. Despite the fact that the traditional fluorosulfate modification strategies rely on rational site-specific design[3] or the warhead conjugation process following phage display[14] , our technology innovates by incorporating the noncanonical amino acid FSY at random positions during *in vitro* translation using degenerate codon libraries (Fig. 1). This enables *de novo* screening of covalent macrocyclic peptides, dramatically expanding screening throughput and diversity. High-salt wash steps during screening efficiently remove non-covalently bound peptides, improving selection efficacy. In the NGS results, the top 10 candidates occupied over 70% of total sequencing quantity, which shared high level of peptide sequence similarity (Fig. 2D). As the top of the list, CP-N1-N_3 performed robust covalent linkage to target protein Nectin-4 (Fig. 2G and Fig. 3B), and the covalent PDC derived from this moiety, CP-N1-MMAE, demonstrated high potency in killing target cells (Fig. 4B). These findings prove the high efficiency

and accuracy of our screening platform.

The past decade has seen significant advances in SuFEx chemistry, enabling robust covalent modification of both small molecules and biologics. Small molecule fluorosulfates can be efficiently synthesized through late-stage modification of phenolic precursors[7], while genetic code expansion techniques permit site-specific incorporation of fluorosulfonyl amino acid into proteins[21], However, fluorosulfate modification remains challenging in peptide synthesis. To address compatibility with SPPS, we implemented a protection/deprotection strategy for precise tyrosine modification without compromising cyclization (Fig. 2E). This synthetic breakthrough enables downstream production of screened covalent macrocyclic peptides, completing the integrated workflow. Furthermore, C-terminal modifications—for example, azide or alkyne as bioorthogonal handles—allow versatile functionalization *via* click chemistry (Fig. 2E). We exemplify this with fluorescent dye-labeled covalent peptides and cytotoxic PDCs. Additional applications could include covalent peptide-radionuclide conjugates (PRCs) and targeted protein degradation platforms[3].

As a high-value oncology target, Nectin-4's tumor-selective expression profile renders it an ideal candidate for developing ADCs and PDCs[33]. Enfortumab vedotin, the first-in-class Nectin-4-targeting ADC, demonstrated significant overall survival benefit in a phase III trial for advanced urothelial carcinoma, securing full FDA approval in 2021[34]. Despite the considerable promise of Nectin-4-targeted therapies, clinical translation of PDCs faces substantial challenges. The underwhelming clinical data for zelenectide pevedotin (BT8009), Bicycle therapeutics' Nectin-4-targeted peptide–drug conjugate, in the Duravelo-1 phase 1/2 study reveal fundamental challenges associated with conventional PDC therapeutics[35]: (i) inadequate non-covalent binding affinity leading to low tumor accumulation; (ii) short target occupancy due to the absence of covalent modification. Consequently, developing covalent macrocyclic peptide-PDCs, leveraging irreversible binding to enhance tumor targeting and drug delivery efficiency, offers a promising strategy to overcome these limitations and provide novel therapeutic solutions for Nectin-4-overexpressing cancers. In our

study, we designed covalent PDC CP-N1-N_3, which performed effective target cancer cell killing (IC_{50} = 43.45 ± 4.00 nmol/L) (Fig 4B). In contrast to the previously mentioned ADC, enfortumab vedotin, our covalent PDC, with its lower molecular weight (~4 kDa), may offer superior tumor penetration. Additionally, CP-N1-MMAE demonstrates high stability, with a half-life ($t_{1/2}$) of 4.4 h in mouse serum, comparable to the bicycle peptide-based PDC BT8009 (Fig. S10). Thus, further structural optimization of these covalent PDCs could yield next-generation Nectin-4-targeting anti-tumor therapeutics.

3. Conclusions

In summary, we established a comprehensive workflow for screening and synthesizing fluorosulfate-containing covalent macrocyclic peptides. This led to the discovery of two potent covalent peptide binders, CP-N1-N_3 and CP-N9-N_3, which bound Nectin-4 with high specificity and efficacy *via* SuFEx click reaction. Therapeutically, our engineered covalent PDC CP-N1-MMAE effectively induced apoptosis in Nectin-4-expressing cells, demonstrating their significant potential as next-generation antitumor therapeutics targeting Nectin-4. Furthermore, our high-throughput covalent peptide screening methodology is readily applicable to diverse target proteins, providing a powerful platform for developing novel covalent therapeutics.

4. Experimental

4.1. Materials and instruments

Unless otherwise stated, chemical synthesis reagents were purchased from commercial sources including Leyan, Bidepharm, Innochem and GL Biochem. All solvents were reagent grade or HPLC grade (Innochem or Adamas). LC–MS spectra were performed on a Waters SQ Detector 2 mass spectrometer coupled to an Acquity ultra performance liquid chromatography (UPLC) system (Waters, UPLC–MS, Singapore). Purity analysis was carried out on Waters 2998 using a Waters XBridge® BEH C-18 (4.6 mm × 150 mm, 2.5 μm) at a flow rate of 1.0 mL/min for analytical HPLC (Waters, Arc-HPLC, Singapore). Purification of peptides on a semi-preparative scale was performed

on a Hanbon (Jiangsu Hanbon Science and Technology Co., Ltd., NU3000C, Huai'an, China) using ChromCore Prep C18 OBD column (5 μm, 120 Å, 21.2 mm × 250 mm) at a flow rate of 10 mL/min. All peptides were separated by RP-HPLC using acetonitrile with 0.1% (*v/v*) TFA with water as mobile phases.

4.2. Synthesis of macrocyclic peptides and PDCs

Synthesis was performed manually on Rink Amide MBHA resin (Bidepharm, BD216754, Shanghai, China) under the standard Fmoc protocol. Detailed synthetic procedures and characterization of purified covalent macrocyclic peptides are provided in Supporting Information.

Add DBCO-Val-Cit-PAB-MMAE (1.1 equiv.) to the *N*, *N*-dimethylformamide (DMF) solution of macrocyclic peptide for 2 h at room temperature. The peptides were purified by preparative RP-HPLC.

4.3. Cell lines and cell culture

MCF-7 cells were purchased from the CellCook (Guangzhou Cellcook Biotech Co., Ltd., catalog# CC0302, Guangzhou, China) and MDA-MB-468 cells were purchased from the Procell (Procell Life Science&Technology Co., Ltd., catalog# CL-0290, Wuhan, China). Fetal bovine serum (FBS) and Dulbecco's modified eagle medium (DMEM) medium were purchased from Gibco (Thermo Fisher Scientific, USA). Non-essential amino acid (NEAA), MEM medium and insulin were purchased from CellCook (Guangzhou Cellcook Biotech Co., Ltd., catalog# CM1008L, CM2015 and CM1007, Guangzhou, China). MDA-MB-468 cells were maintained in DMEM plus 10% FBS and penicillin, streptomycin. MCF-7 cells were cultured in MEM plus 10% FBS and penicillin, streptomycin with 10 μg/mL insulin and 1× NEAA. All cell lines were cultured at 37 °C and 5% CO_2 unless otherwise stated.

4.4. Preparation of unnatural aminoacyl-tRNA

Aminoacylation was performed by mixing 5 mmol/L ^{ClAc}f-CME or FSY-CME with 600

mmol/L $MgCl_2$, 20% DMSO, 25 μmol/L eFx and 25 μmol/L initiator $tRNA^{fMet}_{CAU}$ or elongator $tRNA^{AsnE2}_{CAU}$ and 50 mmol/L HEPES-KOH (pH 7.5). The mixture was incubated for 2 h on ice. The resulting aminoacyl-microhelix/tRNA was purified by ethanol precipitation. Pellets were washed twice with 70% ethanol containing 0.1 mol/L sodium acetate (pH 5.2), frozen with liquid N_2 and stored at –80 °C.

4.5. mRNA display for Nectin-4 binding peptide screening

The selection strategy of mRNA display was conducted as previously described[36,37]. Briefly, DNA libraries were transcribed *in vitro* to generate cognate mRNA libraries, which were ligated to a puromycin linked oligonucleotide. Ribosomal synthesis of the macrocyclic peptide library from the puromycin-linked mRNA library was performed using the PURExfrex 2.0 kit (GeneFrontier Corporation, Kashiwa-shi, Japan), with a custom "Solution I" supplemented with 19 amino acids (-Met), ^{ClAc}f aminoacylated initiator $tRNA^{fMet}_{CAU}$ and FSY aminoacylated $tRNA^{AsnE2}_{CAU}$. Following translation, the resulting mRNA-peptide library was reverse transcribed to generate peptide-mRNA/cDNA libraries, which were panned against 200 nmol/L biotinylated human Nectin-4 ECD immobilized on magnetic beads. The magnetic beads were washed three times with PBS containing 0.01% Tween-20 (PBS-T) followed by two washes with 5 mol/L guanidine hydrochloride on ice and three times with PBS-T to eliminate residual guanidine hydrochloride. Then the fused peptide-mRNA/cDNA was isolated from the beads, with cDNA amplified by PCR, purified by ethanol precipitation and transcribed as above to produce the enriched mRNA library for the next round of selection.

For the second and subsequent rounds of selection, three iterative counter-selections were used to remove peptides with affinity for the streptavidin beads. The final enriched cDNA was processed into Illumina-compatible libraries with VAHTS ssDNA Library Prep Kit (Vazyme, catalog# ND620, Nanjing, China), followed by sequencing performed by Azenta (Nanjing, China) using a next-generation sequencer (Illumina, NovaSeq 6000150PE, USA).

4.6. Surface plasmon resonance (SPR)

SPR experiments were performed using a Biacore 1K and CM5 chips (Cytiva, USA). Experiments were performed at 25 °C in PBS-T. Nectin-4 ECD (50 μg/mL, Sino Biological, catalog# 19771-H08H, Beijing, China) was fixed to RU ~900. A 5-point double dilution series was prepared for each peptide. For covalent binding peptides, a single-cycle kinetic experiment with a contact time of 30 s (short time) or 800 s (long time) and a dissociation time of 200 s was performed at a flow rate of 30 μL/min. For non-covalent binding peptides, a multi-cycle kinetic experiment with a contact time of 60 s and a dissociation time of 60 s was performed at a flow rate of 30 μL/min. Between cycles, the chip was regenerated according to the manufacturer's protocol. Kinetic and affinity analyses were performed using Biacore 1K Evaluation software (Cytiva, USA).

4.7. In-gel fluorescent crosslinking test

For labeling, 1 μmol/L Nectin ECD protein (Nectin-1, catalog# PV1-H5223-100ug; Nectin-2, catalog# PV2-H52E2-100ug; Nectin-3, catalog# PV3-H52E4-100ug; Nectin-4, catalog# NE4-H52H3-100ug, ACRO Biosystems, Beijing, China) was incubated with the indicated concentrations of each chemical probe for annotated time at 37 °C. After protein labeling, 10 μL of resulting mixtures were added to 1 μL of freshly prepared 50 μmol/L DBCO-Cy3 in DMSO. Protein samples were analyzed by SDS-PAGE (4%–12 %) running at 180 V in an electrophoresis chamber under the ambient temperature. In-gel fluorescence was visualized using a chemiluminescence imaging system (Tanon Science and Technology, Tanon 5200, Shanghai, China) followed by staining using Coomassie.

4.8. Immunofluorescent imaging

For testing the covalent binding of peptides, 10 μmol/L Cy3-conjugated peptides were separately added to MDA-MB-468 cells, which were cultured at 37 °C and 5% CO_2 in the dark for 4 h, followed by washed with weak washing buffer (Hank's Balanced Salt Solution, HBSS, pH 7.4) or strong washing buffer (500 mmol/L NaCl, 3% Tween-20,

100 mmol/L glycine, pH 3.0) for three times at room temperature for 10 min.

For testing the tubulin dynamics, MDA-MA-468 cells were incubated with different concentration of PDCs (0, 0.1, 0.5 and 1 μmol/L) at 37 °C for 24 h, followed by fixation with 4% formaldehyde and permeabilization with 0.1% Triton X-100 in 1× PBS. Then cells were stained with anti-tubulin antibody (1:1000, Biodragon, catalog# B1052-50 μL, Suzhou, China), Alexa Fluor. 568-conjuagted Goat anti-Mouse IgG (H+L) (1:1000, Thermo Fisher Scientific, catalog# A11004, USA) and Hoechst 33258 (1:1000, Beyotime, catalog# C1011, Shanghai, China).

All fluorescence was visualized on a Zeiss LSM 880 Confocal Laser Scanning Microscope (ZEISS, Germany) using a 20× objective. The IF imaging results were processed by ZEISS ZEN (ZEISS, Germany).

4.9. Western blotting

MDA-MB-468 cells were seeded in 12-well plates and incubated at 37 °C, 5% CO_2 for 24 h. PDCs were diluted from a 20 mmol/L stock solution to 0, 0.1, 0.5,1, 5 and 10 μmol/L and added to cells, and then incubated for 24 h. After cell processing, cells were collected and lysed by RIPA lysis buffer (Beyotime, catalog# P0013, Shanghai, China) containing protease inhibitors (Beyotime, catalog# SC0078, Shanghai, China). Proteins were separated by SDS-PAGE and performed Western blotting against target proteins caspase-3 (Cell Signaling, catalog# 9662S, Boston, USA), cleaved caspase-3 (Cell Signaling, catalog# 9661T, Boston, USA), PARP (Cell Signaling, catalog# 9542T, Boston, USA), *β*-actin (Beyotime, catalog# AF0003, Shanghai, China) and the secondary antibody (Beyotime, catalog# A0208, A0216, Shanghai, China). The protein bands were scanned on an imaging system with an Enhanced Chemiluminescence Kit (Beyotime, catalog# P0018, Shanghai, China). The results were processed by Image J (National Institutes of Health, USA).

4.10. Fluorescent activated cell sorting (FACS)

For testing the endocytosis of fluorescent dye-conjugated covalent peptides, MDA-

MA-468 cells were incubated with different concentration of CP-N1-Cy3, CP-N9-Cy3 or NP-N7-Cy3 (0, 0.1, 0.5, 1, 5 and 10 μmol/L) at 37 °C for 4 h. Then cells were collected and resuspended in 1× PBS and then quantified the Cy3 signals by NovoCyte@ flow cytometer (ACEA Biosciences, USA).

For testing the cell apoptosis induced by PDCs, MDA-MA-468 cells were incubated with different concentration of PDCs (0, 0.1, 0.5, 1, 5 and 10 μmol/L) at 37 °C for 24 h. Then cells were collected and resuspended in 1× PBS and then stained with the Annexin V-FITC/PI kit (Aladin, catalog# A266226-50T, Shanghai, China). Stained cells were quantified for the FITC and PI signals by NovoCyte@ flow cytometer. The FACS results were processed by FlowJo v10 (BD Biosciences, USA).

4.11. PDC stability test

To test the stability, 100 μmol/L PDCs (CP-N1-MMAE, CP-N9-MMAE or NP-N7-MMAE) were dissolved in 95% mouse serum (Biosharp, catalog# BL1053A, Hefei, China), and incubated at 37 °C for different time (0, 1, 2, 3, 6 and 12 h). Serum proteins were removed by addition with equal volume of acetonitrile and centrifugation. Retained PDCs were monitored by RP-HPLC (Waters 2998, USA).

4.12. Cell viability test

Cells were cultured in 96-well plates with 100 μL of medium at a density of 10^4 per well. Following a 72 h treatment with the indicated PDCs at different concentrations (0, 0.001, 0.003, 0.01, 0.03, 0.1, 0.3, 1, 3 and 10 μmol/L), cell counting kit-8 (CCK-8) solution (APExBIO, catalog# K1018, Shanghai, China) was added and incubated for 2 h at 37 °C. The viability of cells was evaluated by measuring absorbance at 450 nm.

Acknowledgments

We are grateful for the financial support from the CAMS Innovation Fund for Medical Sciences (CIFMS) (2021-I2M-1-026, 2021-I2M-3-001, 2023-I2M-2-006, China), the 2024 China Industrial Technology Infrastructure Public Service Platform Project

(GN2024-31-4700) and the Nonprofit Central Research Institute Fund of Chinese Academy of Medical Sciences (2022RC350-08, China). The cartoon diagrams in figures were generated using Biorender.com.

Author contributions

Rui Wang, Huixin Luo and Ruixuan Wang designed the research. Ruixuan Wang, Siqi Ran, Jiabei Guo and Da Hu carried out the experiments and performed data analysis. Xiang Feng, Jixia zhou, Zhanzhi Zhang, Futian Liang, Jiamin Shang, Lingxin Bu, Kaiyi Wang and Junyi Mao participated part of the experiments. Da Hu, Jiabei Guo, Jixia zhou, Zhanzhi Zhang, Futian Liang, Jiamin Shang, Lingxin Bu, Kaiyi Wang and Junyi Mao provided experimental drugs and quality control. Huixin Luo, Ruixuan Wang, Siqi Ran, Jiabei Guo and Da Hu wrote the manuscript. Rui Wang, Huixin Luo, Ruixuan Wang and Siqi Ran revised the manuscript. All of the authors have read and approved the final manuscript.

Conflicts of interest

The authors declare no conflicts of interest.

Reference

1 Muttenthaler M, King GF, Adams DJ, Alewood PF. Trends in peptide drug discovery. *Nat Rev Drug Discov* 2021;**20**:309-25.

2 Wang L, Wang N, Zhang W, Cheng X, Yan Z, Shao G, et al. Therapeutic peptides: current applications and future directions. *Sig Transduct Target Ther* 2022;**7**:48.

3 Xiao Y, He Z, Li W, Chen D, Niu X, Yang X, et al. A covalent peptide-based lysosome–targeting protein degradation platform for cancer immunotherapy. *Nat Commun* 2025;**16**:1388.

4 Wang N, Yang B, Fu C, Zhu H, Zheng F, Kobayashi T, et al. Genetically encoding fluorosulfate-L-tyrosine to react with lysine, histidine, and tyrosine *via* SuFEx in proteins *in vivo*. *J Am Chem Soc* 2018;**140**:4995-9.

5 Mortenson DE, Brighty GJ, Plate L, Bare G, Chen W, Li S, et al. "Inverse drug discovery" strategy to identify proteins that are targeted by latent electrophiles as exemplified by aryl fluorosulfates. *J Am Chem Soc* 2018;**140**:200-10.

6 Dong J, Krasnova L, Finn MG, Sharpless KB. Sulfur(VI) fluoride exchange (SuFEx): another good reaction for click chemistry. *Angew Chem Int Ed Engl* 2014;**53**:9430-48.

7 Cui XY, Li Z, Kong Z, Liu Y, Meng H, Wen Z, et al. Covalent targeted radioligands potentiate radionuclide therapy. *Nature* 2024;**630**:206-13.

8 Shi Y, Yun Y, Wang R, Liu Z, Wu Z, Xiang Y, et al. Engineering covalent aptamer chimeras for enhanced autophagic degradation of membrane proteins. *Angew Chem Int Ed Engl* 2025;**64**:e202425123.

9 Sun W, Wang N, Liu H, Yu B, Jin L, Ren X, et al. Genetically encoded chemical crosslinking of RNA *in vivo*. *Nat Chem* 2023;**15**:21-32.

10 Zhang H, Han Y, Yang Y, Lin F, Li K, Kong L, et al. Covalently engineered nanobody chimeras for targeted membrane protein degradation. *J Am Chem Soc* 2021;**143**:16377-82.

11 Yu B, Li S, Tabata T, Wang N, Cao L, Kumar GR, et al. Accelerating PERx reaction enables covalent nanobodies for potent neutralization of SARS-CoV-2 and variants. *Chem* 2022;**8**:2766-83.

12 Zheng M, Chen FJ, Li K, Reja RM, Haeffner F, Gao J. Lysine-targeted reversible covalent ligand discovery for proteins *via* phage display. *J Am Chem Soc* 2022;**144**:15885-93.

13 Chen S, Lovell S, Lee S, Fellner M, Mace PD, Bogyo M. Identification of highly selective covalent inhibitors by phage display. *Nat Biotechnol* 2021;**39**:490-8.

14 Wang S, Faucher FF, Bertolini M, Kim H, Yu B, Cao L, et al. Identification of covalent cyclic peptide inhibitors targeting protein-protein interactions using phage display. *J Am Chem Soc* 2025;**147**:7461-75.

15 Iskandar SE, Chiou LF, Leisner TM, Shell DJ, Norris Drouin JL, Vaziri C, et al. Identification of covalent cyclic peptide inhibitors in mRNA display. *J Am*

Chem Soc 2023;**145**:15065-70.

16 Lan T, Peng C, Yao X, Chan RST, Wei T, Rupanya A, et al. Discovery of thioether-cyclized macrocyclic covalent inhibitors by mRNA display. *J Am Chem Soc* 2024;**146**:24053-60.

17 Goto Y, Katoh T, Suga H. Flexizymes for genetic code reprogramming. *Nat Protoc* 2011;**6**:779-90.

18 Cao L, Wang L. Biospecific chemistry for covalent linking of biomacromolecules. *Chem Rev* 2024;**124**:8516-49.

19 Klauser PC, Chopra S, Cao L, Bobba KN, Yu B, Seo Y, et al. Covalent proteins as targeted radionuclide therapies enhance antitumor effects. *ACS Cent Sci* 2023;**9**:1241-51.

20 Cao L, Wang L. New covalent bonding ability for proteins. *Protein Sci* 2022;**31**:312-22.

21 Goto Y, Suga H. The RaPID platform for the discovery of pseudo-natural macrocyclic peptides. *Acc Chem Res* 2021;**54**:3604-17.

22 Liu X, Malins LR, Roche M, Sterjovski J, Duncan R, Garcia ML, et al. Site-selective solid-phase synthesis of a CCR5 sulfopeptide library to interrogate HIV binding and entry. *ACS Chem Biol* 2014;**9**:2074-81.

23 Chen W, Dong J, Li S, Liu Y, Wang Y, Yoon L, et al. Synthesis of sulfotyrosine-containing peptides by incorporating fluorosulfated tyrosine using an Fmoc-based solid-phase strategy. *Angew Chem Int Ed Engl* 2016;**55**:1835-8.

24 Zhou H, Mukherjee P, Liu R, Evrard E, Wang D, Humphrey JM, et al. Introduction of a crystalline, shelf-stable reagent for the synthesis of sulfur(VI) fluorides. *Org Lett* 2018;**20**:812-5.

25 Berdan VY, Klauser PC, Wang L. Covalent peptides and proteins for therapeutics. *Bioorg Med Chem* 2021;**29**:115896.

26 London N. Covalent proximity inducers. *Chem Rev* 2025;**125**:326-68.

27 Liu Y, Han X, Li L, Zhang Y, Huang X, Li G, et al. Role of Nectin-4 protein in cancer (Review). *Int J Oncol* 2021;**59**:93.

28 Fabre Lafay S, Monville F, Garrido-Urbani S, Berruyer Pouyet C, Ginestier C, Reymond N, et al. Nectin-4 is a new histological and serological tumor associated marker for breast cancer. *BMC Cancer* 2007;**7**:73.

29 Gong L, Zhao H, Liu Y, Wu H, Liu C, Chang S, et al. Research advances in peptide–drug conjugates. *Acta Pharm Sin B* 2023;**13**:3659-77.

30 Ma J, Wang X, Hu Y, Ma J, Ma Y, Chen H, et al. Recent advances in augmenting the therapeutic efficacy of peptide–drug conjugates. *J Med Chem* 2025;**68**:9037-56.

31 Wang Y, Cheetham AG, Angacian G, Su H, Xie L, Cui H. Peptide–drug conjugates as effective prodrug strategies for targeted delivery. *Adv Drug Deliv Rev* 2017;**110-111**:112-26.

32 Li Q, Chen Q, Klauser PC, Li M, Zheng F, Wang N, et al. Developing covalent protein drugs *via* proximity-enabled reactive therapeutics. *Cell* 2020;**182**:85-97 e16.

33 Li K, Zhou Y, Zang M, Jin X, Li X. Therapeutic prospects of nectin-4 in cancer: applications and value. *Front Oncol* 2024;**14**:1354543.

34 Challita Eid PM, Satpayev D, Yang P, An Z, Morrison K, Shostak Y, et al. Enfortumab Vedotin antibody-drug conjugate targeting Nectin-4 is a highly potent therapeutic agent in multiple preclinical cancer models. *Cancer Res* 2016;**76**:3003-13.

35 Mudd GE, Scott H, Chen L, van Rietschoten K, Ivanova-Berndt G, Dzionek K, et al. Discovery of BT8009: a Nectin-4 targeting bicycle toxin conjugate for the treatment of cancer. *J Med Chem* 2022;**65**:14337-47.

36 Wu Y, Bertran MT, Joshi D, Maslen SL, Hurd C, Walport LJ. Identification of photocrosslinking peptide ligands by mRNA display. *Commun Chem* 2023;**6**:103.

37 Kawamura A, Munzel M, Kojima T, Yapp C, Bhushan B, Goto Y, et al. Highly selective inhibition of histone demethylases by *de novo* macrocyclic peptides. *Nat Commun* 2017;**8**:14773.

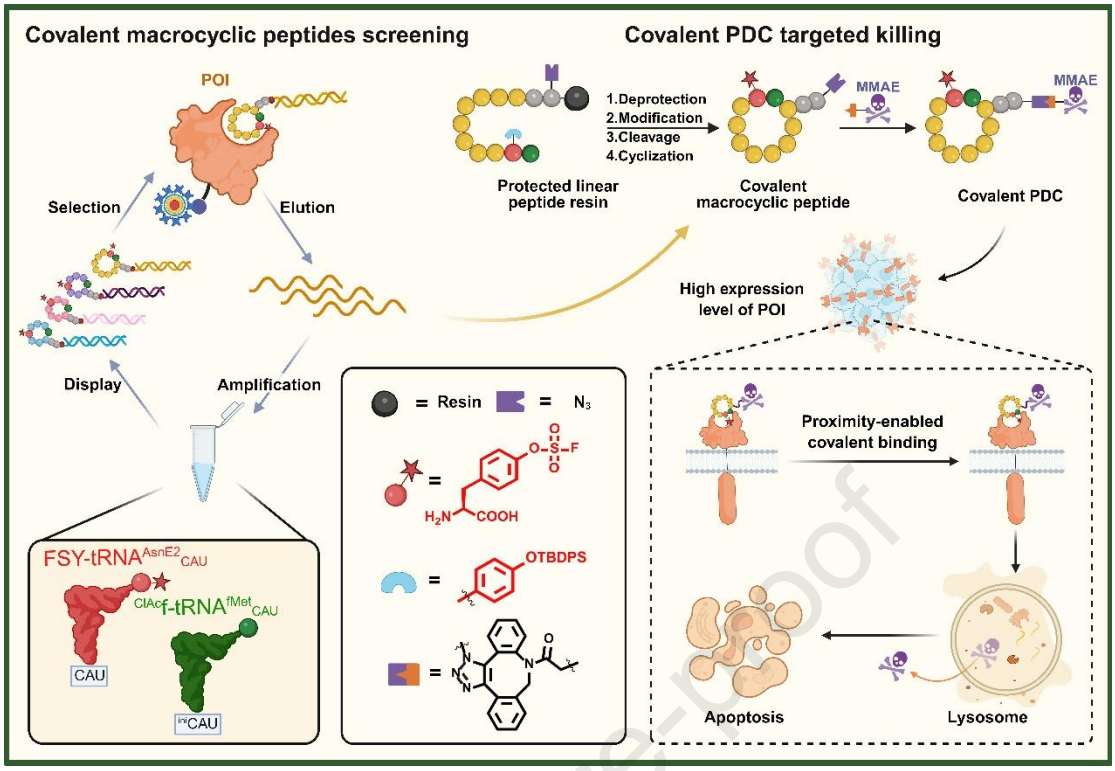

Figure 1 Schematic illustration of covalent macrocyclic peptide screening and antitumor PDC development *via* mRNA display. FSY is incorporated into peptides *via* the FIT system to generate high-diversity mRNA display libraries. Following multiple rounds of selection, top-ranking candidates are identified by next-generation sequencing. Leading candidates are synthesized *via* solid-phase peptide synthesis (SPPS) and utilized to construct covalent PDCs by conjugating to cleavable linkers and cytotoxic payloads. The resulting covalent PDCs can stably bind their target on the cell surface, undergo endocytic trafficking to lysosomes, and release their cytotoxic payload intracellularly to induce apoptosis in target cells.

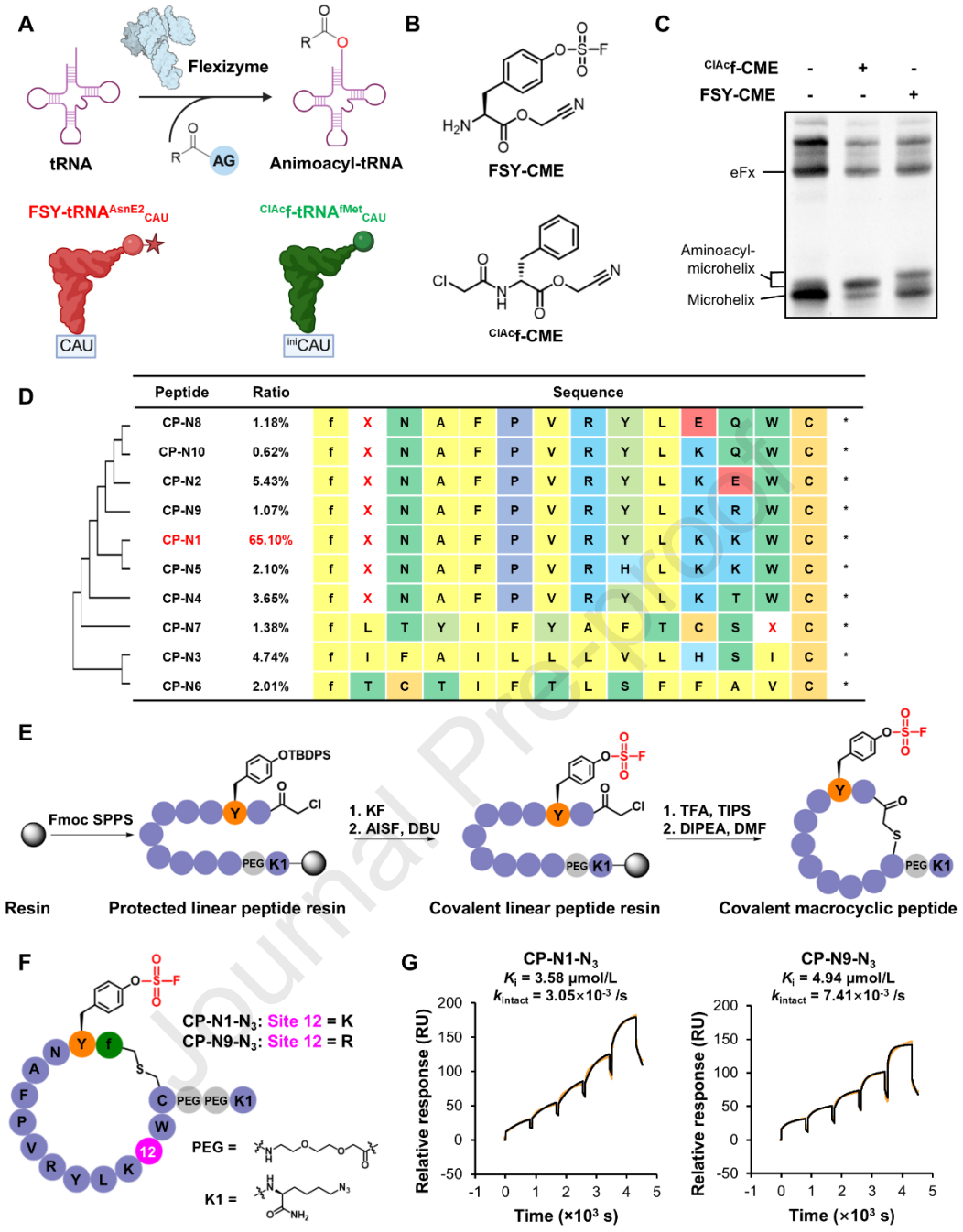

Figure 2 Selection, identification, and preparation of macrocyclic peptide candidates. (A) Scheme diagram of tRNA unnatural aminoacylation by the FIT system. (B) Structures of two unnatural amino acid substrates used for *in vitro* translation, FSY-CME (top) and ^{ClAc}f-CME (bottom). (C) Flexizyme-assisted loading of FSY-CME and ^{ClAc}f-CME onto truncated tRNA (mhRNA) assessed by PAGE; yields were determined by band intensity ratio. (D) Top 10 peptide candidates identified in NGS results. Left was the evolution tree by phylogeny analysis, "f" = D–Phe, and "X" = FSY. (E) Synthesis routine of covalent macrocyclic peptides. (F) Structure of azide-modified

covalent macrocyclic peptides. (G) Single-cycle kinetics SPR sensorgrams of Nectin-4 ECD with covalent macrocyclic peptides, CP-N1-N_3 or CP-N9-N_3.

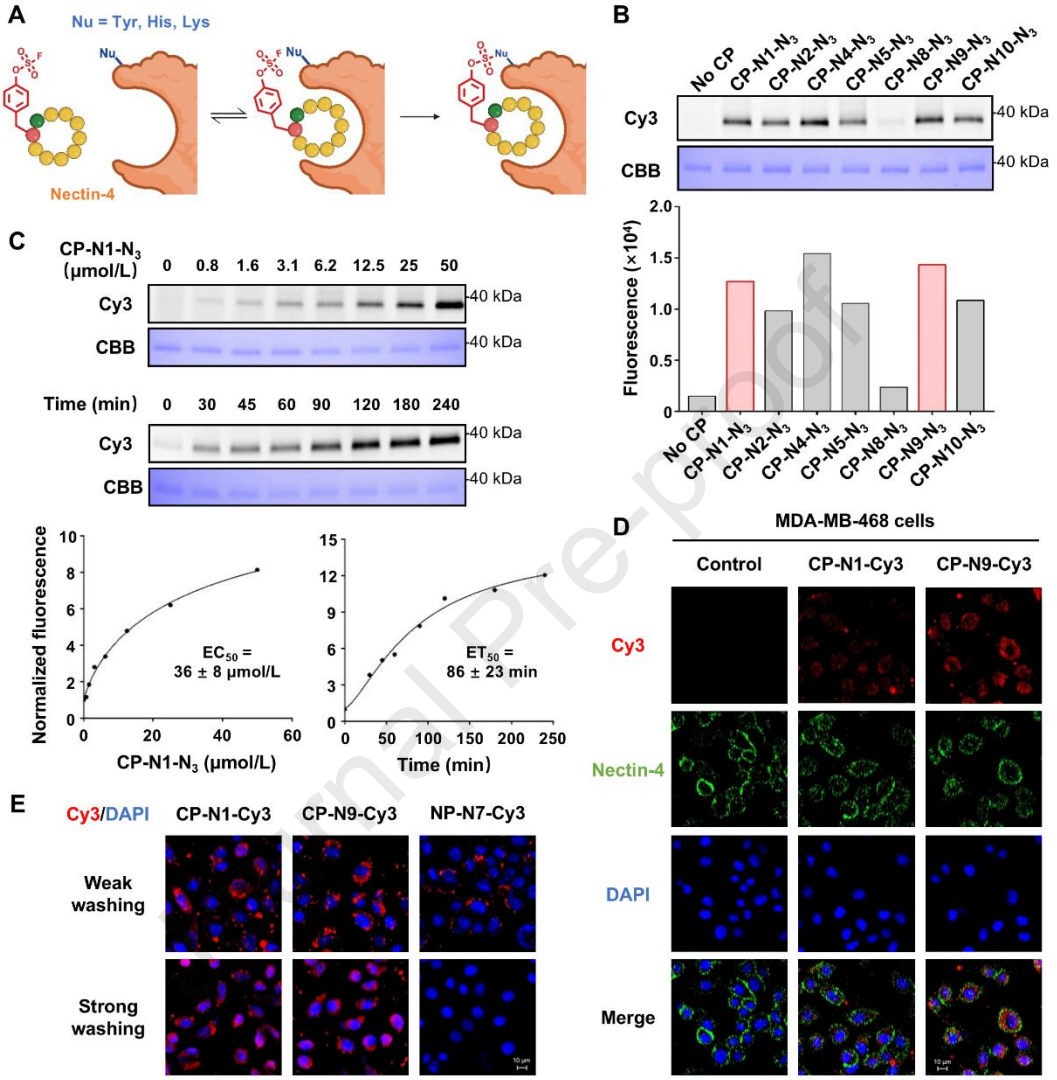

Figure 3 Verification of the covalent binding of macrocyclic peptides to Nectin-4. (A) Scheme diagram of proximal covalent binding between macrocyclic peptides and Nectin-4. (B) In-gel fluorescent imaging of the Nectin-4-macrocyclic peptide covalent binding product. Nectin-4 ECD (1 μmol/L) was incubated with peptides (50 μmol/L) at 37 °C for 24 h, followed by the click reaction with DBCO-Cy3 for fluorescent imaging (top) and Coomassie brilliant blue staining (middle). Cy3 fluorescent signals were quantified by Image J (bottom), and CP-N1-N_3 and CP-N9-N_3 were finally chosen as peptide candidates (red bars). (C) In-gel fluorescent imaging of dose- and time-dependent labeling of CP-N1-N_3 binding to Nectin-4 ECD. Nectin-4 ECD was

separately treated with CP-N1-N_3 at the indicated concentration for 4 h or with 10 μmol/L CP-N1-N_3 for different time intervals, followed by the click reaction with DBCO-Cy3. (D) Immunofluorescent cell imaging of Cy3-conjugated peptides binding to MDA-MB-468 cells. MDA-MB-468 cells were treated with 10 μmol/L Cy3-conjugated peptides at 4 °C for 1 h. Scale bar = 10 μm. (E) Irreversible binding of covalent peptides to the Nectin-4 on MDA-MB 468 cells. MDA-MB-468 cells were treated with 10 μmol/L Cy3-conjugated peptides at 37 °C for 3 h, followed by washing with weak washing buffer or strong washing buffer 3 times. Scale bar = 10 μm.

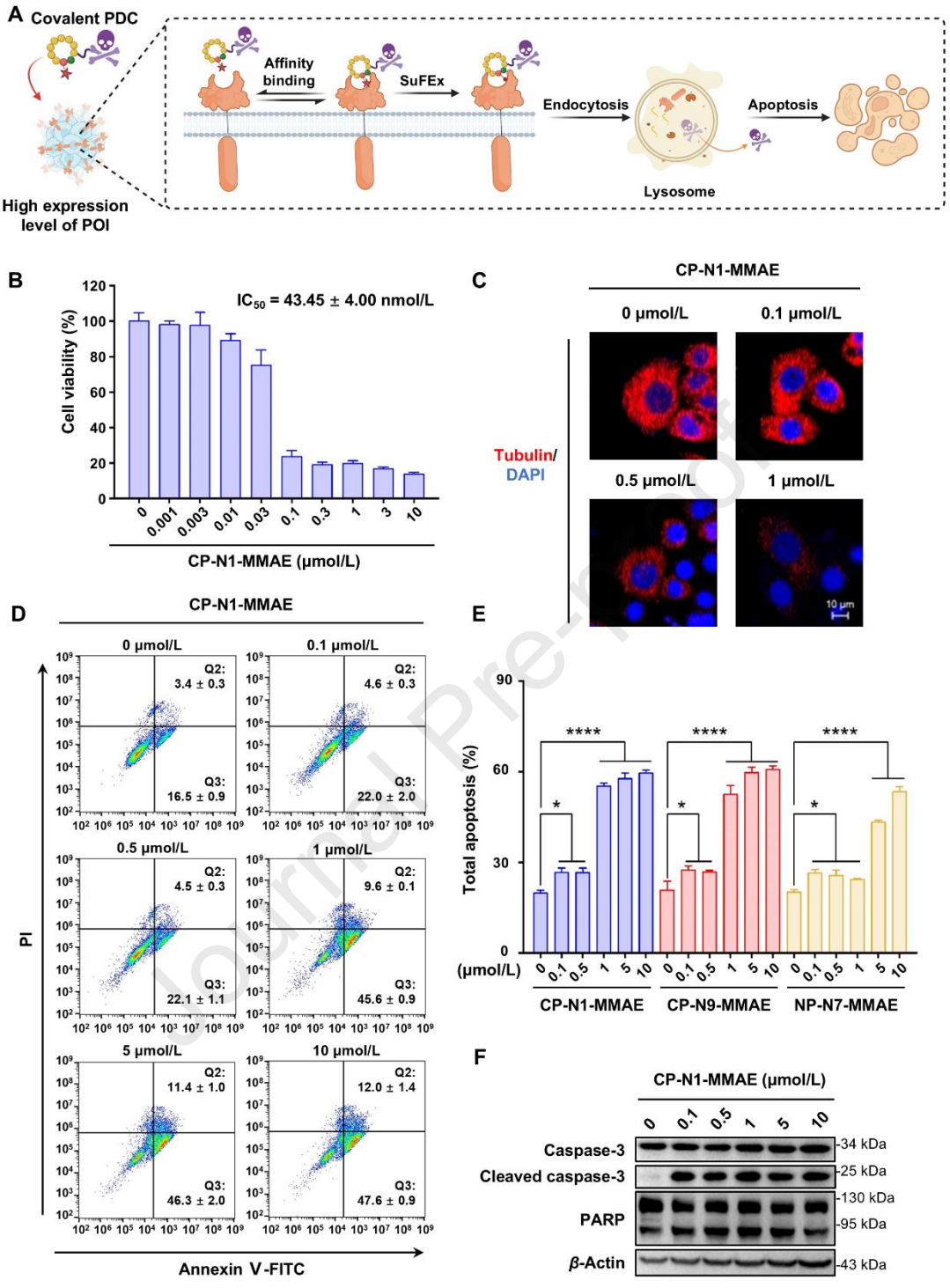

Figure 4 Evaluation and mechanistic analysis of tumor apoptosis induced by covalent PDCs. (A) Scheme diagram of covalent PDC-induced target cell killing, including CP-N1-MMAE and CP-N9-MMAE. (B) Cell viability test after the incubation of CP-N1-MMAE. MDA-MB-468 cells were treated with CP-N1-MMAE at the indicated concentration at 37 °C for 72 h, followed by detecting cell viability by CCK-8 assay. Quantification data were normalized to the signal of the group without incubation. Data

are presented as mean ± SD (n = 6). (C) Disruption of tubulin organization induced by CP-N1-MMAE. MDA-MB-468 cells were treated with CP-N1-MMAE at the indicated concentration in culturing medium at 37 °C for 24 h. The red signals represent tubulin, and the blue signals represent the nuclear. Scale bar = 10 μm. (D) Cell apoptosis induced by CP-N1-MMAE. MDA-MB-468 cells were treated with CP-N1-MMAE at the indicated concentration at 37 °C for 24 h, and then cells were stained with Annexin V/PI for FACS detection. The Q2 area represents cells at late apoptosis, and the Q3 area represents cells at early apoptosis. Data are presented as mean ± SD (n = 3). (E) Total apoptosis of MDA-MB-468 cells after PDC incubation. Data are presented as mean ± SD (n = 3). *P<0.05. ****P<0.0001. (F) The cleavage of caspase-3 and PARP induced by CP-N1-MMAE. MDA-MB-468 cells were treated with CP-N1-MMAE at the indicated concentration at 37 °C for 24 h, with cell lysate detected by western blotting.